Coronary stenting: from optical coherence tomography to fluid dynamic simulations

C. Chiastra[1*], E. Montin[2*], F. Burzotta[3], L. Mainardi[2], F. Migliavacca[1]

***Abstract*—The presence of stents within coronary arteries alters the hemodynamic condition. Computational fluid dynamics (CFD) simulations offer the possibility to study local hemodynamics of a stented artery to identify the stimuli of in-stent restenosis, i.e. the local reduction of lumen size after stent deployment. The results of CFD simulations are more accurate when the analyses are performed with a model reproducing real *in vivo* conditions. For this purpose, optical coherence tomography (OCT) is a promising tool to reconstruct 3D geometries of stented coronary arteries, due to its higher resolution compared to the other imaging techniques.**

In the present work a reconstruction method of stented coronary bifurcation geometrical models starting from OCT images was developed. An OCT exam performed in a stented coronary bifurcation silicone sample was considered. The vessel and the stent were reconstructed separately, and then they were merged together. Vessel reconstruction was performed with a semi-automatic process: the main branch was reconstructed by fitting the lumen boundary with ellipses and subsequently by creating a mesh of the vessel; the side branch was created like an ideal cylinder. Stent struts were identified with an automatic algorithm; then, the stent was reconstructed in a manual way. After the creation of the 3D geometry of the bifurcation, a transient fluid dynamic simulation was carried out. CFD results showed that the highest risk of restenosis is located in the region near the bifurcation.

I. Introduction

RESTENOSIS after stent implantation remains a persistent clinical problem in the treatment of atherosclerosis through percutaneous coronary intervention [1]. The mechanisms of restenosis are not completely understood, but direct endothelial and smooth muscle cell damage, reduced compliance and alterations in the distributions of wall shear stress (WSS) have been implicated as potential triggering events that stimulate the excessive growth of tissue inside the stented region [2],[3].
Obtaining a full comprehension of the mechanism of in-stent restenosis is extremely important. The presence of the stent inside a coronary artery alters the hemodynamics, leading to recirculation or stagnation zones which are associates with low WSS. It is reasonably assumed that risk of restenosis is higher in the regions characterized by low WSS [4],[5] and high values of oscillatory shear index (OSI) and relative residence time (RRT) [6],[7]. Computational fluid dynamics (CFD) offers the possibility to study the local hemodynamics of the stented artery to identify stimuli for restenosis. Results of a CFD simulation are more accurate when the numerical analysis is performed with a model reproducing condition resembling the reality. Only in few studies image-based geometrical models of coronary arteries were reconstructed for CFD simulations [8]–[11]. However, in those studies only the stent or the arterial wall were obtained from imaging data, never both of them at the same time.

Currently, optical coherence tomography (OCT) is a promising imaging technique for coronary arteries, due to its high resolution (10-20 μm) and the possibility to detect both the stent and the vessel wall [12],[13]. Thanks to these characteristics, OCT seems to be a promising tool to reconstruct 3D geometries of stented coronary arteries. The aim of this work is to develop a reconstruction method of stented coronary bifurcation geometrical models starting from OCT images. The geometry obtained through this method is subsequently used to perform a CFD simulation to quantify WSS and the other near-wall quantities and to correlate them to the process of restenosis.

II. Materials and Methods

A. Geometrical model reconstruction

An OCT exam was performed *in vitro* in an ideal silicone model of stented coronary bifurcation. In this model a Multi-Link Vision stent (Abbott Laboratories, Abbott Park, IL, USA) was deployed following the provisional side branch stenting technique. OCT images were acquired through a Fourier-Domain C7-XR™ Imaging System (St. Jude Medical, Inc., St. Paul, MN, USA) at the Policlinico Gemelli hospital in Rome, Italy. The images were stored in the DICOM medical imaging standard file and then they were processed in Matlab v.R2010a (MathWorks Inc. – Natick, MA, USA).

In Fig. 1 the general workflow of the reconstruction method of the stented coronary artery is shown. The first step of the method consisted in the image pre-processing:

C. Chiastra and F. Migliavacca are with LaBS, Department of Chemistry, Materials and Chemical Engineering "Giulio Natta", Politecnico di Milano, Milan, Italy.

E. Montin and L. Mainardi are with the Department of Electronics, Information and Bioengineering, Politecnico di Milano, Milan, Italy.

F. Burzotta is with the Department of Cardiovascular Medicine, Università Cattolica del Sacro Cuore, Rome, Italy.

F. Migliavacca is the corresponding author (phone: +3923994316; fax: +3923994286; e-mail: francesco.migliavacca@polimi.it)

* Authors equally contributed to the work

978-1-4799-3163-7/13/$31.00 ©2013 IEEE

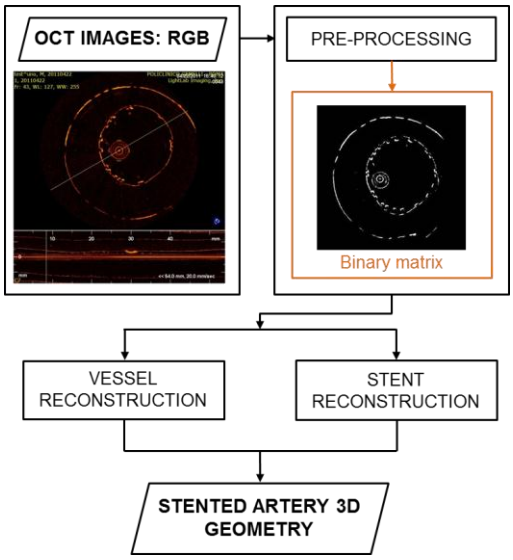

Fig. 1. General workflow of the reconstruction method of a stented coronary bifurcation model from OCT images.

i) images were converted to grayscale; *ii*) the lower part of each image, which contains the longitudinal section of the vessel, was cut because not necessary for the vessel reconstruction; *iii*), specific thresholds were applied to remove the noise, and *iv*) the images were converted into a logical matrix.

After the pre-processing, the reconstruction method is characterized by two separated parts that allow the creation of the 3D stented artery geometry: the vessel and the stent reconstruction.

Vessel reconstruction

To fit the vessel with the model (ellipse) a step for the stent removal is needed. A series of automatic operations were performed in Matlab for each slice as reported in Fig. 2.The algorithm started with a raw identification of the stent struts combining "opening" and "closing" operations on a binarized image with threshold set to the measured noise level of the techniques. Then, a subtraction was done between the logical matrix, resulted from the pre-processing step, and the new matrix containing the struts. The result was a matrix in which the vessel wall and the stent struts were separated, the majority of the struts were removed. The external edge of the vessel was removed (this part was present because the OCT exam was performed into a silicone model and not *in vivo*). The next step was the elimination of the catheter. Since its position is fixed in all the images, it was removed by assigning a value of zero to all the pixels of that region. Afterwards, the lumen border was fitted with an ellipse, which represents a good approximation for the ideal silicone coronary artery cross-section. Repeating the operations for all the slices, a point cloud representing the vessel was obtained.

The points were imported in the CAD software Rhinoceros v.4.0 Evaluation (McNeel & Associates, Indianapolis, IN, USA) (Fig. 2). Starting from them, a surface mesh was created obtaining the geometry of the main branch. The side branch was created as an ideal cylinder since OCT was performed only in the main branch. Its dimensions and orientation were known. Finally the main branch and side branch were merged together.

Stent reconstruction

An algorithm which automatically identifies the position of the stent struts was developed in Matlab (Fig. 3). In order to obtain images that contain only struts, each slice was segmented by applying a "fuzzy c-means" clustering (FCM) filter the inner zone of the fitted vessels.

FCM is a clustering method which perform the probability of one piece of data to belong to two or more clusters or seeds based on some features [17], in this work these features were the RGB values of OCT image .

FCM was applied using three seeds which represent the vessels, the struts and the background, this filter was initialized to the RGB values of these three labels. For each pixels the probability to belong to each labels was calculated.

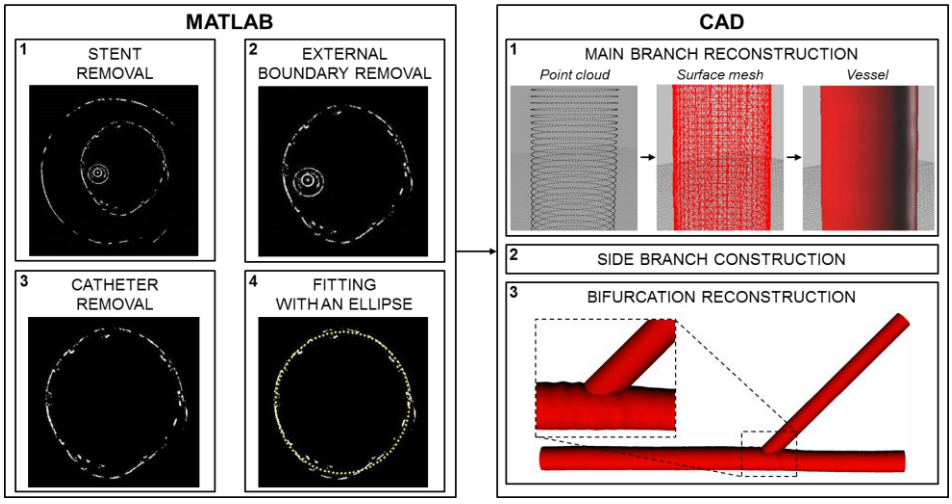

Fig. 2. Diagram of the workflow used for the vessel reconstruction.

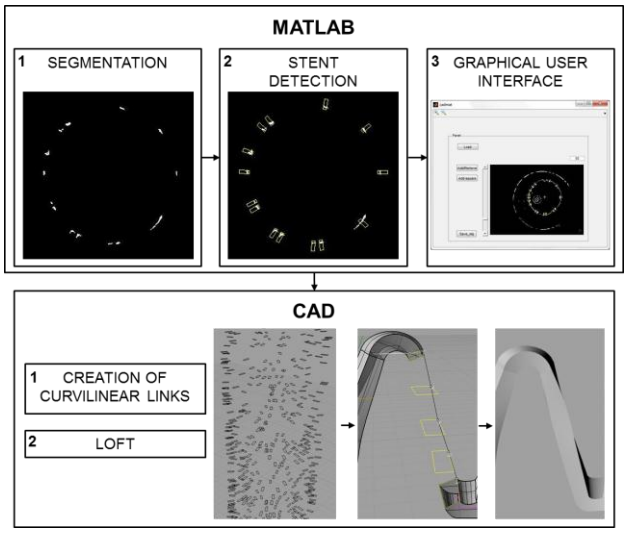

Fig. 3. Diagram of the workflow used for the stent reconstruction.

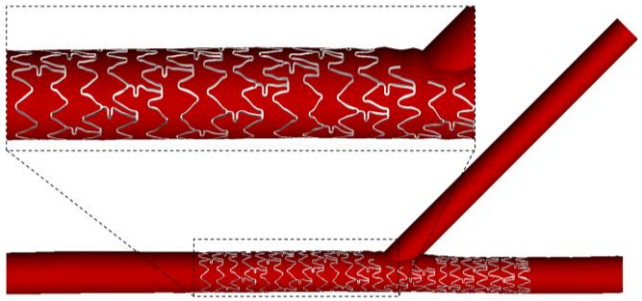
Fig. 4. Final 3D geometry of the stented coronary bifurcation obtained through the reconstruction method starting from OCT images.

Subsequently in order to correctly mark each pixel with only one of the three labels a defuzzyification step was performed, in this step the pixels were labeled according to the maximal probable mark. After that a logical matrix was created of the area defined as struts and for each region a rectangle was imposed. This rectangle had a size of the real strut and was rotated so that the radius defined from the center of the ellipse and the shorter side of the rectangle was perpendicular to the latter.

In the next step, the user, through a graphical user interface, could visualize all the slices, adding/removing rectangles if they were not correctly identified. When the creation of the rectangles was finished, the algorithm produced an object file that contains all the rectangles of the slices in the correct longitudinal position.

In the final step, the object file was opened in the CAD software (Fig. 3), where all the rectangles were manually linked through loft operations, following the geometry of the Multi-Link Vision stent and using curvilinear links extracted from the CAD model of the stent.

B. Fluid dynamic analyses

The 3D geometry obtained from OCT images using the reconstruction method was imported into ANSYS ICEM CFD 14.0 (ANSYS Inc., Canonsburg, PA, USA) to create the computational grid. In order to assure accurate results in the stented region (area of interest), the mesh size was chosen after a mesh independence study. Three tetrahedral meshes with an increasing element number (4,800,565, 7,923,535 and 10,751,884 elements) were created to perform steady-state simulations. The second mesh was chosen as the percentage difference with the finest mesh in terms of WSS was lower than the chosen threshold (0.5%). Then, in order to reduce the number of elements and to increase the computational speed, a hybrid discretization of the arterial volume was created, following the method developed in [14]. The number of elements of the hybrid mesh was 7,291,683, about 8% lower than the full tetrahedral mesh, implying an increase of computational speed.

A transient fluid dynamic simulation was carried by means of ANSYS FLUENT 14.0. Blood was assumed as an incompressible, non-Newtonian fluid, with the viscosity varying according to the Carreau's model [8].

At the inlet, a time-dependent blood flow was applied, referring to [15]. At the outlets, a flow split was imposed. The values of the flow split were calculated applying the relation between flow-rate and vessel diameter as in [16]. Wall and stent were assumed to be rigid and were defined with a no-slip condition. A coupled solver was used with a second-order upwind scheme for the momentum spatial discretization. Under-relaxation factors of 0.15 were used for pressure and momentum. Convergence criterion for continuity and velocity residual was set to 10^{-6}.

The results of the CFD simulation were analyzed in terms of velocity pattern, time-averaged wall shear stress (TAWSS), OSI and RRT. The definition of these quantities can be found in [8]. The TAWSS was investigated not only by means of contour maps but also with a quantitative analysis. Since values of WSS lower than 0.4 Pa are considered as critical for the process of restenosis [4],[5], the percentage area of the stented region exposed to TAWSS lower than 0.4 Pa was calculated. Moreover, the histogram of the area distribution of TAWSS was analyzed.

III. Results and Discussion

The 3D geometrical model of the stented coronary bifurcation reconstructed from OCT images using the method developed in this work is shown in Fig. 4. Struts appear deformed because of the balloon expansion, and well apposed overall.

Concerning fluid dynamic results, Fig. 5a shows the velocity magnitude contour map over a longitudinal plane at the peak of flow rate. In accordance to [9], it is possible to observe that the velocity profiles are skewed toward the carina, resulting in lower velocity in the region opposite to it. Moreover, there are recirculation zones near the struts, as found in [12], and stagnation areas in the bifurcation region, where the struts alter the blood flow toward side branch. In addition, the contour map of shear rate, comparable with the

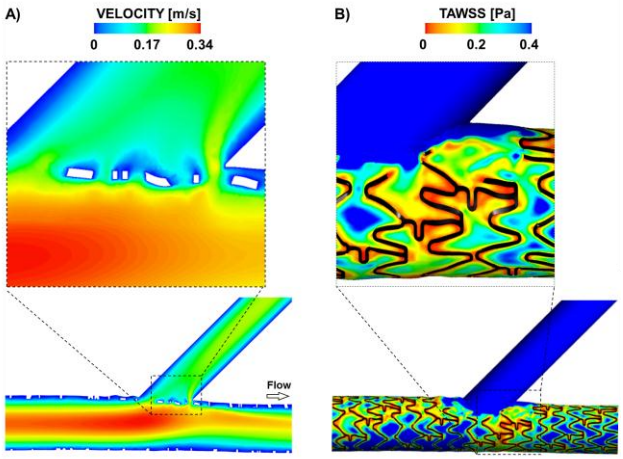

Fig. 5. A) Contour map of velocity magnitude at the peak of flow rate in the middle plane. The magnification shows the stagnations zones near the stent struts of the bifurcation region. B) Contour map TAWSS. The magnification shows the low WSS values in the region close to the bifurcation.

results obtained in [9], shows higher values of shear rate (critical zones) are located in proximity of the entrance of side branch.

Figure 5b points out that low TAWSS (< 0.4 Pa) are located next to the struts and the bifurcation region, according with results in [8]. Quantitative analysis of TAWSS shows that the percentage area with TAWSS < 0.4 Pa was 72.8%. This result is confirmed by the TAWSS distribution, characterized by a mean value of 0.32 Pa and positive values of skewness and kurtosis. This indicates that the distribution of TAWSS is skewed to the right (wider area with TAWSS values lower than the mean) and more peaked if related with the normal distribution.

IV. Conclusion

The present work shows a method for the reconstruction of a stented coronary artery bifurcation model from OCT images. The geometry obtained through this method was investigated by means of a CFD simulation, in order to quantify near-wall quantities and to correlate them with restenosis process. Although this is an ideal arterial vessel with a stent, results confirmed that the highest risk of restenosis is located in the region near the bifurcation. Among the limitations we mention that this method is only tested on a phantom data with a simple geometry without a quantitative validation.

The reconstruction method might be used to obtain 3D geometries of stented coronary arteries for CFD analyses that better approximate the *in vivo* conditions; in this way, the fluid dynamic results should be more reliable than the results obtained with idealized models.

References

[1] S. Garg and P.W. Serruyus, "Coronary stents: current status", *J. Am. Coll Cardiol*, vol. 56 (10 Suppl), pp. S1-42, 2010.

[2] J.F. LaDisa Jr, D.A. Hettrick, L.E. Olson, I. Guler, E.R. Gross, T.T. Kress, J.R. Kersten, D.C. Warltier, P.S. Pagel, "Stent implantation alters coronary artery hemodynamics and wall shear stress during maximal vasodilation", *J Appl Physiol*, vol. 93, pp. 1939-1946, 2002.

[3] J.M. Garasic, E.R. Edelman, J.C. Squire, P. Seifert, M.S. Williams, C. Rogers, "Stent and artery geometry determine intimal thickening independent of arterial injury", *Circulation*, vol. 101, pp. 812-818, 2000.

[4] J.F. LaDisa Jr, L.E. Olson, R.C. Molthen, D.A. Hettrick, P.F. Pratt, M.D. Hardel, J.R. Kersten, D.C. Warltier, P.S. Pagel, "Alterations in wall shear stress predict sites of neointimal hyperplasia after stent implantation in rabbit iliac arteries", *Am J Physiol Heart Circ Physiol*, vol. 288, pp. H2465-H2475, 2005.

[5] A.M. Malek, S.L. Alper, S. Izumo, "Hemodynamic Shear Stress and Its Role in Atherosclerosis", *J Am Med Assoc*, vol. 282, pp. 2035-2042, 1999.

[6] H.A. Himburg, D.M. Grzybowski, A.L.Hazel, J.A. LaMack, X.M. Li, M.H. Friedman, "Spatial comparison between wall shear stress measures and porcine arterial endothelial permeability", *Am J Physiol Heart Circ Physiol*, vol. 286, pp. H1916-1922, 2004.

[7] Y. Hoi, Y.Q. Zhou, X. Zhang, R.M. Henkelman, D.A. Steinman, "Correlation between local hemodynamics and lesion distribution in a novel aortic regurgitation murine model of atherosclerosis", *Ann Biomed Eng*, vol. 39, pp. 1414-1422, 2011.

[8] C. Chiastra, S. Morlacchi, D. Gallo, U. Morbiducci, R. Cárdenes, I. Larrabide, F. Migliavacca, "Computational fluid dynamic simulations of image-based stented coronary bifurcation models", *J R Soc Interface*, Vol. 10, 20130193, 2013.

[9] N. Foin, R. Torii, P. Mortier, M. De Beule, N. Viceconte, P.H. Chan, J.E. Davies, X.Y. Xu, R. Krams, C. Di Mario, "Kissing balloon or sequential dilation of the side branch and main vessel for provisional stenting of bifurcations: lessons from micro-computed tomography and computational simulations", *JACC Cardiovasc Interv*, vol. 5, pp. 47-56, 2012.

[10] L.M. Ellwein, H. Otake, T.J. Gundert, B.K. Koo, T. Shinke, Y. Honda, J. Shite, J.F. LaDisa Jr, "Optical coherence tomography for patient-specific 3D reconstruction and evaluation of wall shear stress in a left circumflex coronary artery", *Cardiovasc Eng Tech*, vol. 2, pp. 212-227, 2011.

[11] S. Morlacchi, B. Keller, P. Arcangeli, M. Balzan, F. Migliavacca, G. Dubini, J. Gunn, N. Arnold, A. Narracott, D. Evans, P. Lawford, "Hemodynamics and in-stent restenosis: micro-CT images, histology, and computer simulations", *Ann Biomed Eng*, 39, pp. 2615-2626, 2011.

[12] M.U. Farooq, A. Khasnis, A. Majid, M.Y. Kassab, "The role of optical coherence tomography in vascular medicine", *Vasc Med*, vol. 14, pp. 63-71, 2009.

[13] F. Prati, E. Regar, G.S. Mintz, E. Arbustini, C. Di Mario, I.K. Jang, T. Akasaka, M. Costa, G. Guagliumi, E. Grube, Y. Ozaki, F. Pinto, P.W. Serruys, "Expert review document on methodology, terminology, and clinical applications of optical coherence tomography: physical principles, methodology of image acquisition, and clinical application for assessment of coronary arteries and atherosclerosis", *Eur Heart J*, vol. 31, pp. 401-415, 2010.

[14] C. Chiastra, S. Morlacchi, S. Pereira, G. Dubini, F. Migliavacca, "Fluid dynamics of stented coronary bifurcations studied with a hybrid discretization method". *Eur J Mech - B/Fluids*, vol. 35, pp. 76-84, 2012.

[15] J.E. Davies, Z.I. Whinnett, D.P. Francis, C.H. Manisty, J. Aguado-Sierra, K. Willson, R.A. Foale, I.S. Malik, A.D. Hughes, K.H. Parker, J. Mayer, "Evidence of dominant backward-propagating suction wave responsible for diastolic coronary filling in humans, attenuated in left ventricular hypertrophy", Circulation, vol. 113, pp. 1768-1778, 2006.

[16] A.G. van der Giessen, H.C. Groen, P. Doriot, P.J. de Feyter, A.F.W. van der Steen, F.N. van de Vosse, J.J. Wentzel, F.J.H. Gijsen, "The influence of boundary conditions on wall shear stress distribution in patients specific coronary trees", *J Biomech*, vol. 44, pp. 1089-1095, 2011.

[17] J.C. Noordam, W.H.A.M. van den Broek, L.M.C. Buydens, "Geometrically Guided Fuzzy C-Means Clustering for Multivariate Image Segmentation", *Proc. International Conference on Pattern Recognition*, Vol. 1, 2000, pp. 462-465.